21

Water-in-Oil Emulsions in Recovery of Hydrocarbons from Oil Sands

Jan Czarnecki
Edmonton Research Centre, Syncrude Canada Ltd., Edmonton, Alberta, Canada

I. INTRODUCTION

Conventional oil reserves decline all over the world. The same is true for Canada, which is self-sufficient in oil production. Although some oil is imported to eastern Canada, an excess production from the west is sold, mainly to the USA. Overall, Canada's consumption of oil is balanced by its production. However, the current production markedly exceeds new oil discoveries. If this trend continues, in several years Canada would become a net oil importer. Fortunately for the country, huge oil sand deposits in northern Alberta constitute an alternative source of fuels. Oil sands are fluvial, estuarine, and marine deposits of sand saturated with bitumen, a form of heavy oil. Typically, the oil sand ore contains about 9—13 wt% bitumen, the rest being a mixture of silica sand and fine clays.

Figure 1 shows the location of major oil sand deposits. In the blown-up insert, which is a simplified map of Alberta, one of the western Canadian provinces, the locations of oil sand deposits are marked in black. In the Athabasca region, the ore is located close to the surface allowing for surface mining. Two major commercial plants operate here, some 40 km north of the city of Fort McMurray. Both operating companies, Syncrude Canada Ltd and Suncor Energy Inc., Oil Sands, use surface mining and water-extraction methods to recover the bitumen. Several new projects are on the drawing board, the most advanced is a new mine to be operated by Shell Canada. In the Cold Lake and Peace River areas, where the oil is covered with a thicker layer of overburden, in-situ enhanced oil-recovery methods are used for commercial bitumen recovery.

The bitumen extracted from oil sands is too heavy to be shipped directly to the market. Most of the bitumen produced is upgraded by a combination of standard refinery Technologies. Both Syncrude and Suncor use coking as the main primary upgrading method. It is followed by hydrotreatment, eventually to produce light sweet blends that are sold at premium. A major pipeline links Fort McMurray area with the North American pipeline system. About 15% of Canadian oil production (or consumption) comes from the Athabasca Oil Sands. Producers from Cold Lake and Peace River use a diluent, mainly natural gas condensate, to pipeline the dilute bitumen produced to refineries where it is upgraded to make commercial products. The total contribution of oil sands hydrocarbons to Canadian oil production currently exceeds 25% and is projected to bypass the 50% mark in the first decade of the twenty-first century.

The total reserves of hydrocarbons contained in the Alberta Oil Sands are huge. As shown in Figure 2, the total

Figure 1 Location of oil sand deposits in northern Alberta.

amounts of hydrocarbons locked in the oil sands that are recoverable using surface mining followed by water-extraction Technologies, are slightly higher than the total oil reserves of Saudi Arabia. However, the total hydrocarbon reserves contained in the oil sands located in northern Alberta are higher than the total known oil reserves of all OPEC countries combined.

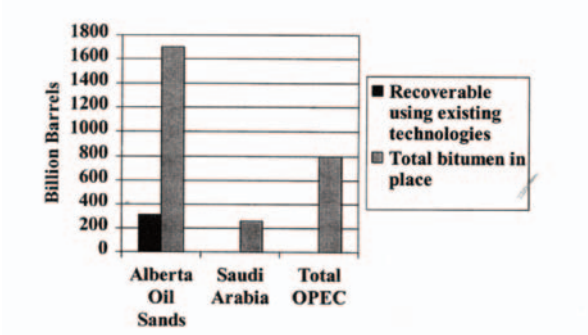

Figure 2 Reserves of hydrocarbons locked in oil sands compared to other major oil sources.

The oil sand industry has succeeded in remarkable reduction in unit operation costs. In the first half of 1999, the costs of producing a barrel of upgraded synthetic sweet blend from oil sands by surface mining is hovering around Canadian $13, i.e., about US $ 8 (at the current exchange rate). Therefore, even at the low oil prices of late 1998 and early 1999, the industry is making a profit. New emerging technologies are likely to lower further the unit costs to about Canadian $ 10 or so within the next decade. It is thus evident that the oil sand industry is robust enough to become the main source of oil for Canada if not for North America for decades to come. This decline in the unit operating costs is mostly due to the introduction of new technologies in mining, extraction, and upgrading. New technologies were made possible because of extensive research efforts. The specific feature of the oil-sand industry is the need for knowledge, which is generated by joint efforts of industry, academia, and government research facilities. In the following paragraph, the teachnology for

bitumen recovery, as used today, is briefly described.

The ore is primarily mined by a truck and shovel operation. Crushed ore is then mixed with water at the mine front and pumped to the extraction plant. This new hydrotransport technology has been already implemented by both operating plants and is to be utilized by all planned operations. In the pipeline the ore is digested, i.e., the existing lumps are ablated and the bitumen is liberated. The existing operations run the slurry pipelines at about 50°C. In the new planned operations coming on line in 2000, the pipeline temperature is going to be around 25° C, resulting in further reductions in energy use and in unit operating costs. Since the slurry preparation involves dumping the ore into water, screening, and pumping, some air is entrained in the slurry and dispersed into small air bubbles. Additional air is usually introduced to the pipeline. The bubbles collide with liberated bitumen droplets to form stable aggregates. All these processes make the slurry ready for consecutive bitumen separation. This takes place in large, relatively stagnant separation vessels, where the aerated bitumen rises to the surface forming a froth.

The froth contains typically about 60% bitumen, 30% water, and 10% solids. To remove solids and water, the froth is diluted with a diluent, in both existing operations this is locally produced naphtha. Bitumen density is about the same as that of water. Addition of a light solvent lowers the density of the oil phase and, at the same time, lowers its viscosity, making water and solids separation possible. In the froth-treatment operation, scroll and disk centrifuges as well as incline plate settlers (IPSs) are used for cleaning the froth diluted with naphtha. The product, which usually contains less than 2% water and less than 0.4% fine solids, is then fed to upgrading. Here, in the first operation, the diluent is recovered and recycled to froth treatment.

The problem is that the residual water mentioned above contains dissolved salts, mostly sodium chloride, which is then carried to the downstream upgrading operations, creating serious corrosion risks. The salt is coming from the ore, and because of the water recycle, accumulates in the process waters. Most of the water in diluted bitumen is present in the form of relatively large drops and lenses, which are relatively easy to remove in the froth-treatment operation. However, small quantities of water form a very stable emulsion, with a droplet size of about 2—5 μm. Removal of this water is of paramount importance, since excess of chloride salts, after treatment with hydrogen in hydrotreatment, is converted into hydrochloric acid. At the same time organic nitrogen is converted into ammonia. We thus have all the conditions to form volatile ammonium chloride than canmigrate throughout the plant tending to precipitate in cooler and moister places, such as heat exchangers. In summary, the plant integrity depends on effective removal of water emulsified in diluted bitumen.

Pilot tests of conventional electrostatic desalters failed to improve water removal. In an attempt at improving dewatering efficiency, by making changes to the composition and amount of the diluent used for froth treatment, it was discovered that for paraffinic solvents, at sufficiently high diluent-to-bitumen ratio (D/B), a very clean and dry product can be made (1). This observation, first made on a bench scale, was then confirmed in extensive pilot studies. As the result, a new technology, the paraffinic froth-treatment process, was developed. In its future commercial operation, Shell Canada is planning to employ this technology by using natural gas condensate as the source of paraffinic diluent. The paraffinic process seems to have a number of advantages in a 'green field' situation. However, it is as always difficult to implement a new technology in an existing operating plant. Therefore, at Syncrude, several other coping strategies have been implemented ranging from the construction of a third-stage centrifuge plant to a joint research program with the demulsifier supplier, Champion Technologies, to optimize and customize the demulsifiers used in commercial operation. Despite considerable efforts and costs the problem is not yet satisfactorily solved.

There are two issues here —- first, Technological: how to lower the water content in the froth-treatment product, and second, scientific: what makes the water emulsion so stable. In this paper, I will focus on the latter and describe the results of collaborative studies performed by a group of researchers from the NSERC Research Chair in Oil Sands headed by Dr Jacob Masliyah from the Department of Chemical and Materials Engineering, University of Alberta in Edmonton,* CANMET Western Research Centre (Canadian Government research laboratory), and Syncrude's Edmonton Research Centre.

One of the important characteristics of the oil sand industry is that it is unique to Alberta and, contrary to conventional oil which relies on worldwide research activities, there is very little known about the scientific needs of the oil sand industry outside the industry itself. Also, since the main competition to the oil sand industry is conventional oil, there is less need for extensive protection of intellectual property. Those two factors combined create an environment that strongly promotes collaboration in various areas,

* Natural Sciences and Engineering Research Council (NSERC) support in the form of a grant to Dr Jacob Masliyah, the Chairholder of NSERC Research Chair in Oil Sands, is gratefully acknowledged.

but especially in basic, precompetitive research. The material presented in this chapter summarizes the results of such collaborative efforts of the group mentioned above. Efforts were made to make flow of information as easy and boundary between various participating groups as fuzzy as possible.

II. WASHING EXPERIMENTS

There are several hypotheses concerning the source of the water in bitumen emulsion stability. The most common says that the emulsion is stabilized by the asphalthene fraction of the bitumen. The following experiment (1) clearly shows that, although the stabilizers may come from the asphalthene fraction, it is not the whole asphalthene fraction that is responsible for the emulsion stability.

Figure 3 shows the schematic of the washing experiment. First, a solution of bitumen in toluene was prepared. Second, known aliquots of water were blended with the bitumen solution under standardized conditions. The emulsion formed (which we will call the first emulsion) was centrifuged under high rpm to create a clean supernatant. In the next step, 10% of water was blended into the supernatant to form the second emulsion. The stability of this secondary emulsion was studied as a function of the amount of water used to make the first emulsion. It is worth adding that the first emulsion was not broken even at high acceleration. Instead, the emulsion was concentrated at the bottom of the centrifuge cell in the form of a cake without any free water visible. Some of the results of washing experiments are shown in Figure 4.

As the amount of water used to make the first emulsion increases, the stability of the secondary emulsion decreases. This indicates that there is a possibility of exhausting the finite reserve of the material, which is responsible for the high emulsion stability, regardless what this material may

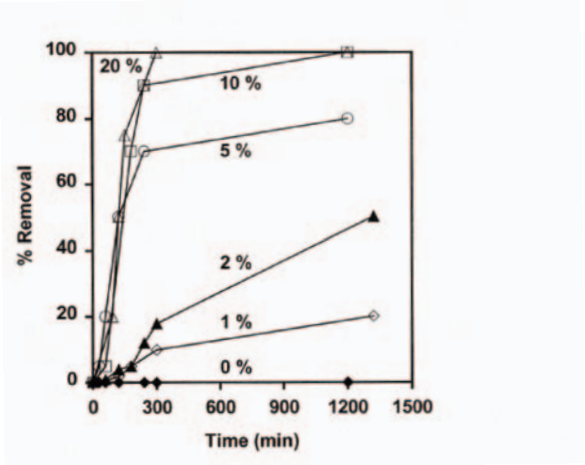

Figure 4 Washing experiments results: percentage of water removed from the secondary emulsion for various amounts of water used to make the first emulsion, or to "wash" the oil.

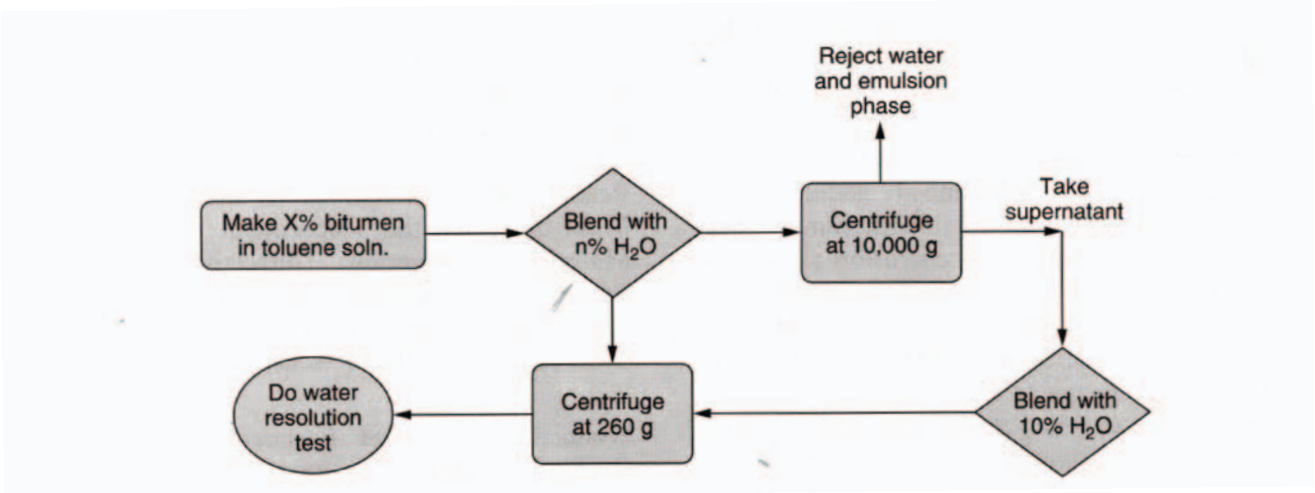

Figure 3 Flow sheet of the washing experiment. Description in the text.

be. It can be seen in the figure that, above the 5% water used to make the first, "washing" emulsion, the stability of the emulsion formed in the second step is already markedly reduced and is only slightly affected by increasing further the amount of washing water. In the first emulsion, most of the droplets are about 3 μm. We can calculate the total surface area of the water droplets in, say, 100 ml of 10% water emulsion. Then, assuming that the thickness of the layer that stabilizes the droplets via a steric mechanism is, say, 20 nm,* and that it has the same density as bitumen (i.e., 1 g/ml), we obtain the mass of the stabilizing layer as about 0.4 g. Since we had 25 g of bitumen in 10 ml toluene solution, this constitutes less than 2% of the bitumen. Now, the asphalthene content in Athabasca bitumen is about 18%. The conclusion is that, if asphalthenes are involved in stabilizing the emulsion, it can only be a small subfraction of the total asphalthene content of the oil.

III. COLLOIDAL COLLIDER: COLLOIDAL FORCES BETWEEN EMULSIFIED WATER DROPLETS

Knowing the interaction forces between emulsified water droplets would help in understanding the reasons for the observed high stability of water in diluted bitumen emulsion. However, studies on liquid/liquid interactions are very limited, especially on forces between microscopic emulsion droplets. Recently, a new force-measuring technique, colloidal particle scattering (CPS), was developed to measure surface forces between micrometer-sized latex particles (2, 3). The apparatus, called a microcollider, is capable of determining forces of 10^{-14}-10^{-12} N, which is several orders of magnitude smaller than those detected by the surface-force apparatus (SFA) or atomic-force microscope (AFM). We performed experiments to measure the interaction forces between two 6.5-μm water droplets in a toluene-based solvent containing a small amount of bitumen.

The basic principles of CPS are described in detail in Ref. 2. In essence, the method is based on generating collisions between two micrometer-sized particles (droplets) under simple shear flow conditions and extracting the force-distance relationships by analyzing the asymmetry of collision trajectories before and after the collision. Figure 5 shows the schematic of the experiment set-up. The measuring cell consists of a fixed, upper wall made of optical glass and a movable bottom forming a gap of about 200 μm. The movements of the cell bottom are controlled by a computer and can be executed either by a joystick or by running a program resulting in the creation of a known shear flow within the cell. A collision is generated by bringing a random droplet in the emulsion, exhibiting Brownian motions, into contact with a previously found droplet attached to the upper cell wall. The collision is observed and recorded through the upper cell wall with a microscope equipped with a CCD camera and a VHS recorder. The image is then analyzed to find the position of the mobile droplet long before and after the collision. All three coordinates of the droplet can be extracted from the image. The x,y coordinates can be deducted from the image directly. The third z coordinate, normal to the plane of observation, can be calculated from the velocity of the droplet in the flow and the known shear rate, crated in the cell. Hydrodynamic considerations show that if there is no net attraction or repulsion between the droplets, the trajectory of the particle should be symmetrical with respect to the stationary droplet. However, if the droplets repel each other the mo-

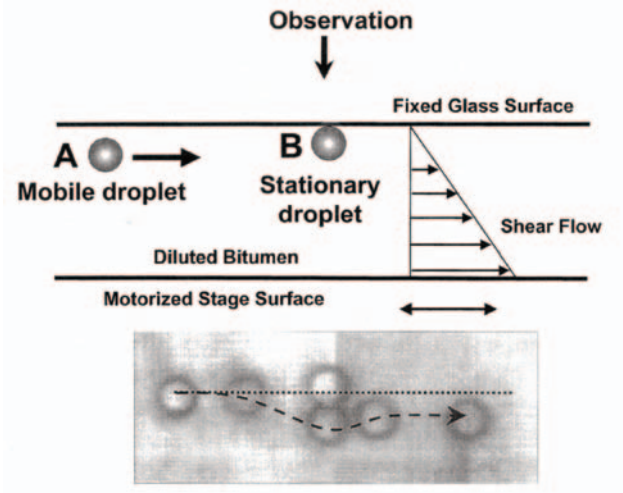

Figure 5 Principle of the colloidal collider method. The shear flow is created between upper fixed plate and the mobile bottom of the cell. The insert shows several consecutive positions of the mobile droplet as it passes around the stationary one. The dotted line depicts a symmetrical trajectory expected when no surface forces exist. The dashed line shows the experimental trajectory indicating a repulsive interaction between the two droplets.

In the following section, dealing with colloidal collider experiments, we present material indicating that the stability is as a result of a nonhomogeneous steric barrier with a thickness varying from 7 to 40 nm.

bile droplet will be pushed away from the stationary one resulting in a shift of its final position (long after collision) versus the initial starting point. A detailed description of the method, including experimental procedure, theoretical basis for calculating the forces from the observed droplet trajectories, and error analysis are given in Refs 2-4.

To estimate colloidal forces acting between the droplets during the collision, x, z coordinates of the initial (x_i, z_i) and final (x_f, z_f) positions of the mobile droplet before and after the collision are needed. When several pairs of x, z coordinates are plotted on a graph a specific "scattering pattern" will appear. This pattern can be analyzed by comparing the experimental final positions with the ones calculated from a theory (2,3), which covers hydrodynamic interactions between the droplets and between the mobile droplet and the wall as well as all external forces acting on the mobile drop, e.g., those described by DLVO theory. Thus, in the calculations, we assume the existence of a certain force described by a certain function of the droplet-droplet separation. The final position of the droplet is then calculated and compared with the experimental results. The best match between experimental and theoretical final droplet positions yields the optimum set of parameters or the optimum force-distance profile.

One of the limitations of the collider method is the requirement of neutral buoyancy of the studied droplets in the medium. To match the density of the solution with that of the water, we mixed 71 wt% toluene with 29wt% dibromobenzene (density 1.95 g/ml). The organic phase also contained 0.04 wt% bitumen extracted from Athabasca oil sand. Emulsion-stability tests showed that dibromobenzene had a negligible effect on the stability.

The experimental results are summarized in scattering diagrams (cf. Figs 6 and 7). The open circles represent initial positions of the mobile droplet (x_j,Z_j) and the solid circles represent final positions (x_f, z_f). Owing to the poor light transmission in a dark bitumen solution, only seven collisions were analyzed.* The initial (open circles) and final (solid circles) droplet positions, numbered from 1 to 7, are shown in the figure. The scattering diagram shows that the final positions do not follow a "ring" pattern, normally observed in previous studies of polystyrene latex particle interactions (2, 4) where the force-distance relationship is consistent for all collisions.

It has been known that water droplets in a bitumen/toluene solution are stable. Since the van der Waals forces between two water droplets are always attractive, a repulsive force is required to stabilize the system.

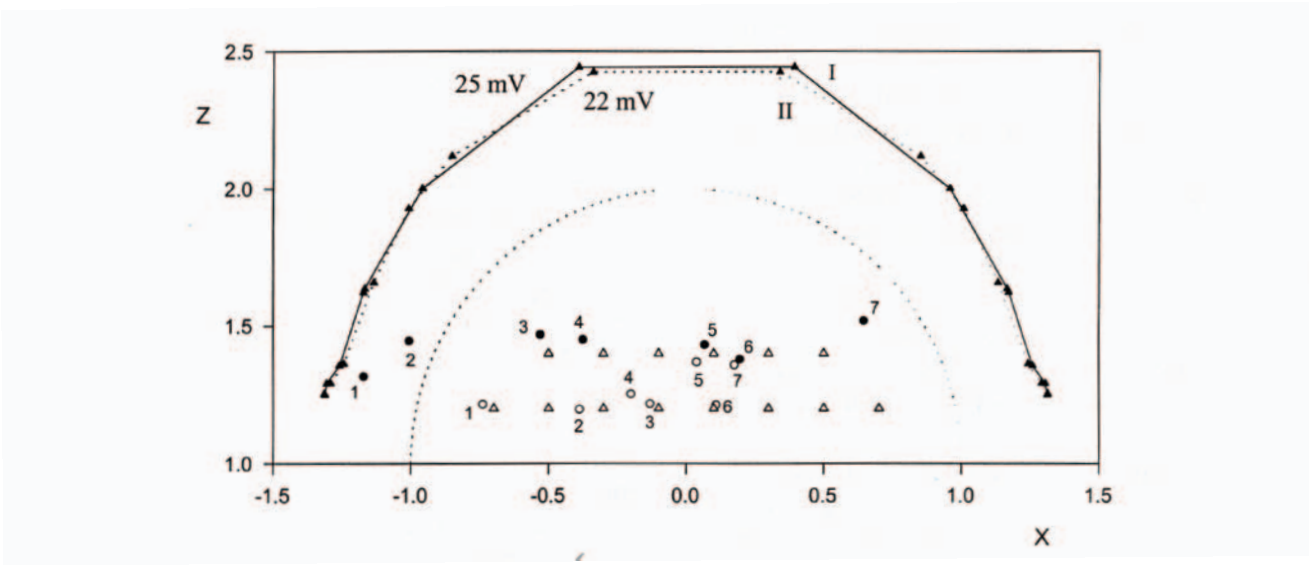

Figure 6 Scattering diagram. Open circles: initial mobile droplet positions; solid circles: final mobile droplet positions. Open and solid triangles are initial and final positions taken for calculating scattering pattern if electrostatic forces were involved for surface potential 22 and 25 mV. Below 22 mV calculations suggested droplet coagulation.

* To enhance the contrast we added 0.01% of fluorescein isothiocyanate to the water. In the second instrument built we use reflected rather than transmitted light illumination and we use a polished stainless steel plate as the bottom of the cell that acts as a mirror. These modifications allowed us to work with solutions containing up to 10% bitumen without any dye in the aqueous phase.

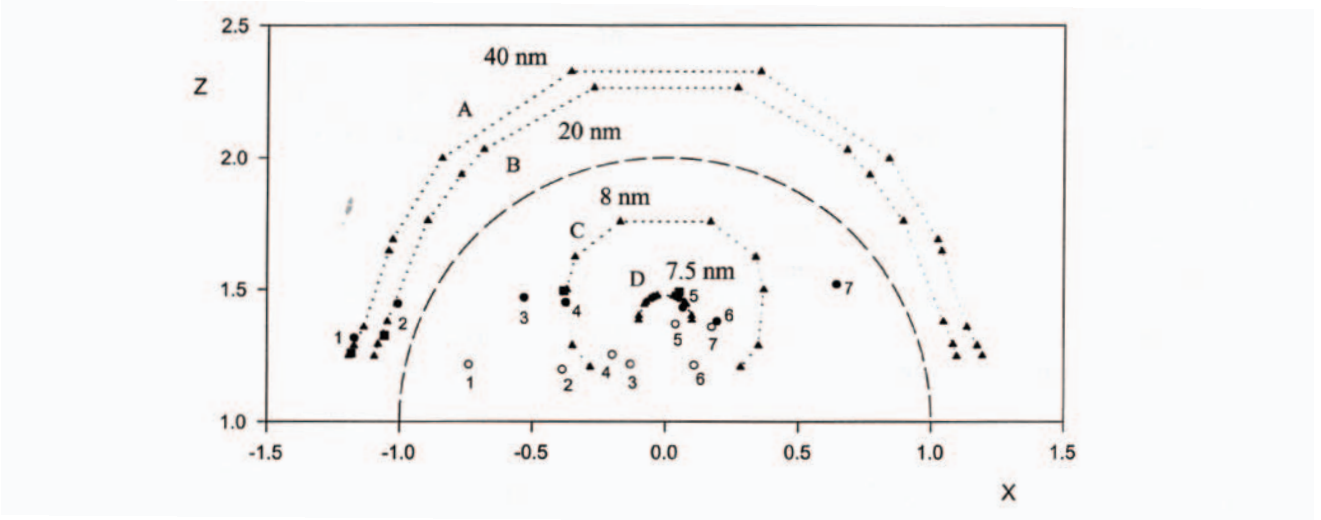

Figure 7 Scattering diagram. Experimental initial and final positions are open and solid circles, respectively; the solid triangles depict final positions for a steric repulsion model with various thicknesses of the steric layer. The initial positions were the same as in Figure 6.

The most common repulsive forces are electrostatic and steric repulsion. The electrostatic interaction in a low dielectric constant organic medium is not fully understand. (We are currently working on a theory based on a cell model.) For the analysis reported herein we assumed that the electrostatic interactions in an organic medium are similar to that in an aqueous system of the same conductivity. The conductivity of our system is about 30 S/m. In an aqueous system, this would be the conductivity of 2×10^6M 1:1 electrolyte (e.g., NaCl). In an organic medium, however, ions are considerably smaller than their hydrated counterparts in water. This increases the equivalent conductivity of ions, so the argument above overestimates the actual ionic strength in an organic medium. Hence, we took a value of 1×10^6M as the ionic strength of our system. We also found that varying this value by one or two orders of magnitude does not change the final results qualitatively. This yields a m value of 70 (k being the Debye parameter and a the drop radius). The large ka value suggests that the double-layer interaction theory might still apply to our nonaqu-eous system. We used a modified Gouy-Chapman theory to calculate the electrostatic force.

Van der Waals forces were calculated on the basis of Hamaker's theory with a retardation function introduced by Schenkel and Kitchener (5). The Hamaker constant of water-toluene-water was taken from Ref. 6. Both the Hamaker constant and the retardation wavelength were kept constant.

Figure 6 gives two theoretical final positions "rings" (solid triangles) with surface potentials of 22 and 25 mV (signs unspecified). They correspond to arbitrarily chosen initial positions marked in the figure with open triangles. When the surface potential was below 22 mV, our calculations indicated that the mobile droplet should be captured permanently to form a doublet, contrary to our observations. It is obvious that the experimental final positions, which are mostly located close to the origin (0.0, 1.0), cannot be explained using the theoretical approach described above, no matter what is the value of the surface potential or ionic strength of the medium.

The steric repulsion mechanism is also difficult tc model in our system. A bitumen/toluene solution itself is a very complex system containing high molecular weight asphaltenes, natural surfactants, and ultrafine particles. These components are very likely to be adsorbed on the water/toluene interface. Due to this complexity, it is hard to model the adsorption layer with a single elastic modulus, as was done for the analysis of poly(ethylene oxide) adsorption layers on latexes (7). However, all steric forces resemble hard-wall interactions. They can be approximately modeled by high-order polynomial functions. We used a simple expression $F_{\text{steric}} = c/h^7$, where h is the separation

distance between two droplets, and c is a constant chosen in such a way that it makes icteric equal to the nonretarded van der Waals force at $h = 2L_S$ (L_S being the adsorption layer thickness). The power of h is arbitrary. The above formula describes a steric force that is zero slightly beyond L_S and increases sharply as the distance L_S is reached. It has been found that the final results are not sensitive to this power as long as it remains reasonably high. Based on this model, in Fig. 7 we plot theoretical final "rings" (solid triangles) using the same initial positions shown in Fig. 6 with open triangles. The scattering diagram shows that the experimental final position of collision 1 is located on ring A and the final position of collision 5 is on ring D. Other final positions located between rings A and D can also be predicted by varying L_S between 7.5 and 40 nm. Therefore, we may state that our experimental results are consistent with the assumption of steric repulsion resulting from a heterogeneous steric layer. Another experimental finding by Yoon et al. (8) indicates that by using a SFA the interaction forces in an inverse system, i.e., bitumen/water/bitumen, resemble polymer/polymer interactions. If we assume that these interactions are caused by hydrophobic parts of the surfactants adsorbed on the bitumen/water interface, it is of no surprise to observe the steric interactions between hydrophobic parts of the same surfactants in a water/bitumen/water system. Error analysis indicated that the error is around 50 and 1% for the maximum and minimum value of L_S, respectively.

The most important message from the colloidal collider experiments is that our results will be consistent with any mechanism in which the repulsive force is decaying much faster than the attractive one (the van der Waals force). A steric force obviously meets this requirement. A well-screened double-layer force would also satisfy this condition at a certain separation h, and the resulting shallow minimum is called a secondary minimum in DLVO theory. However, this requires a high ionic strength (~ 0.01 M) which is not possible in our system. If the actual ionic strength of our system is several orders of magnitude less than the assumed value (10^6M), the electric double layers cannot be fully developed and it is inappropriate to calculate the electrostatic force with a double-layer interaction equation. Although we do not know exactly what form the force equation will take, we know the expression of the Coulomb force, which is the extreme case of electrostatic interactions without screening. It does not decay faster with increasing h than the van der Waals forces. For this reason, it seems that the electrostatic force is unlikely to be the main cause of stabilization in the system studied, although it may play a minor role in addition to the steric stabilization mechanism.

IV. MICROPIPETTE STUDIES: THE INTERFACIAL PROPERTIES OF MICROMETER SIZED WATER DROPLETS IN DILUTE BITUMEN

The conclusion from the previous section was that the remarkable stability of water-in-diluted bitumen emulsions is due to the presence of a complex adsorbed layer at the surfaces of the dispersed droplets. Except for its role as a steric barrier, little is known about the properties of this interfacial layer. New insights were provided by direct, micrometer-scale measurements using the micropipet method, a technique borrowed from biology. It has long been noted that, in macro-scale studies (involving sample sizes of millimeters or larger), structures appearing as "rigid skins" would often form at the crude oil-water interface (9-12). To make connections with emulsion systems, these skin-like structures are often likened to the adsorbed layer formed on the surfaces of micrometer-sized emulsion droplets. Such an extrapolation, however, may not necessarily be valid. For instance, interfacial tension at the emulsion drop surface (including water in crude oil cases) can markedly differ from interfacial tension measured with commonly used macroscale techniques, such as the spinning drop or Du Noüy ring. The difference results from the vastly different surface-to-volume ratios between the experimental setups (13). (It is likely that similar discrepancies exist between interfacial viscous and elastic properties as measured with micro or macro methods.)

The micropipet technique was developed to examine directly the interfacial properties of individual, micrometer-sized emulsion droplets, thus avoiding the extra-polative approach of necessity adopted by macroscale studies. The technique was originally developed as a tool for the biological and biophysical sciences (14-16). We have modified the technique for investigations of interfacial phenomena on individual, micrometer-sized emulsion droplets by using equally small suction pippets. A detailed description of our procedure can be found in Refs. 17 and 27.

A. Emulsion Preparation

In the studies reported in this chapter, the hydrocarbon (continuous) phase of the emulsion was composed of coker feed bitumen, extracted from Athabasca Oil Sand deposit (18). To attain workable viscosities, bitumen is diluted in a 1:1 mixture, by volume, of n-heptane and toluene (both

HPLC grade with no further purification). Such a solvent, which will be called "hep-tol," is chosen to simulate the aromatic/aliphatic ratio of the diluent used in commercial oil sand processing (18). In this work, bitumen contents of the oil phase, denoted by Co, are expressed as volume percentages. Filtered, deionized water was used as the aqueous phase. An emulsion was prepared by adding 100µl of water to 10 ml of diluted bitumen (lvol.% water). The mixture was sonicated for several seconds, creating a macroemulsion of water droplets. Depending on the bitumen concentration and the duration of sonica-tion, the average droplet size was between 5 and 30µm. It was verified that the interfacial tension of the droplets (method of measurement discussed below) reaches an equilibrium value after the first minute of emulsification and remains unchanged for days. In this study, all emulsions were aged for 20 min.

B. Interfacial Tension

As a first application, the micropipet was used to measure the interfacial tensions (IFTs) of individual emulsion drops. As shown in Figure 8, a single water droplet in an oil-continuous emulsion is held at the tip of a suction pipet (note at meniscus inside the capillary). From mechanical equilibrium, the critical pressure P_{cr} needed to draw the water drop into an oilfilled pipet is related to the oil-water interfacial tension σ by

$$\sigma = \frac{P_{cr} R_p}{2(1 - R_p/R_o)} \quad (1)$$

where Rv is the inner radius of the pipette, and R_0 is the radius of the droplet (19). Thus, the interfacial tension on a micrometer-sized emulsion droplet can be evaluated form simple measurements of pressure, and droplet and pipet sizes. This new method of ten-siometry has been verified for emulsion systems consisting of pure liquids (17).

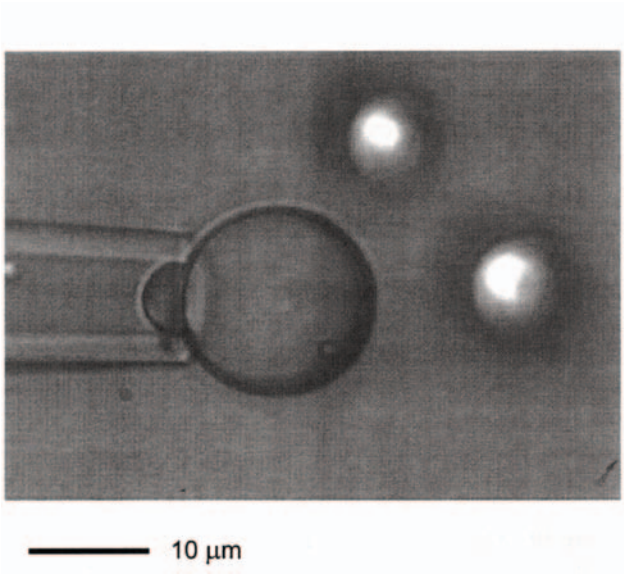

Figure 8 A water droplet held with suction at the end of a micropipet. Note the curved meniscus inside the capillary. The pressure balance allows one to calculate the interfacial tension on an emulsion droplet in situ.

C. Layers at Droplet Surfaces

Micropipet technique can also be used for studies of the adsorbed layer formed on emulsion droplets. Many natural components of crude oil are surface active and will tend to adsorb on the hydrocarbon-water interface (20). Surface excess of the adsorbed material can then be calculated from the Gibbs equation. In our case, we will use the concentration of bitumen in the solvent, since we do not know what is the chemical(s) responsible for droplet stabilization and what its concentration is. We will use the micropipet technique discussed above, to measure true IFT at emulsion drop surfaces.

Figure 9 shows changes in the equilibrium interfacial tension a as the bitumen content Co is varied over four orders of magnitude. Each data point is the average IFT of at least 12 droplets. The error bars extend over two standard deviations. The horizontal line in Fig. 9 represents the IFT between water and pure solvent. Note that Co is the bitumen content prior to emulsion preparation and it may generally be lower at equilibrium. Nevertheless, useful information can still be extracted from two limiting cases: the plateau regime at $C_0 \leq 0.1\%$ and the linear regime at $C_0 \geq 0.5\%$. They correspond to shortages and surpluses of surfactants relative to the available "interfacial sites," respectively.* It can be shown that, in both these limits, C_0 is proportional to the surfactant concentration in the oil phase (17). Assuming diluted bitumen to be an ideal, single-component surfactant solution (a simplistic picture which provides a lumped characterization of crude oil's surface active components), we can apply the Gibbs relation to the data

* Such an observation remains valid despite the lack of precise control of the total interfacial area.

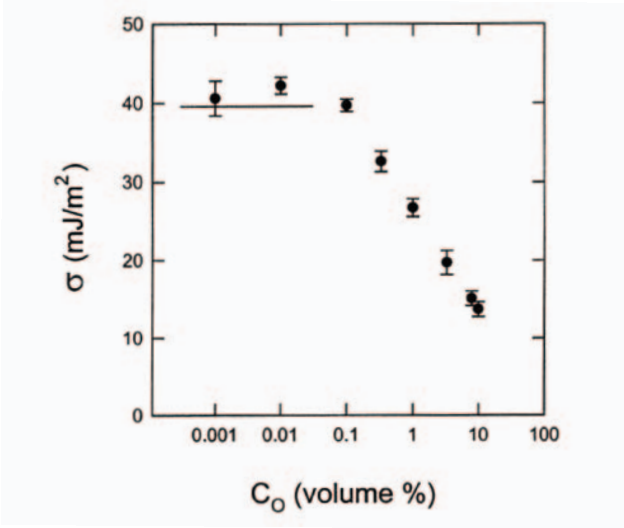

Figure 9 Interfacial tension at water droplets in toluene containing increasing amounts of bitumen. The solid line on the figure represents toluene —- water interfacial tension.

shown in Fig. 9. It can thus be inferred that in the plateau regime ($C_0 \leq 0.1\%$), $\Gamma \approx 0$, i.e., there should be little or no adsorbed material on the droplet surfaces. In the linear regime ($C_0 \geq 0.5\%$), where the droplet surfaces are saturated with surfactants, the area per "site," given by the reciprocal of Γ, is 0.74 nm^2. Our estimate of the molecular cross-section at saturation is about an order of magnitude lower than most literature values (21, 22). The discrepancy may be due to factors such as the type of oil, solvent properties, and water chemistry. In addition, it remains an open question whether the crude oil-water interface in, say, a Du Noüy ring experiment (the most common technique), is structurally similar to the adsorbed layer at the surfaces of emulsified water drops (structures that are directly probed in this study).

D. Mechanical Properties of the Adsorbed Layer

Macroscale studies in the past had pointed to the formation of a "rigid skin" at the crude oil-water interface (9-11). We observed similar structures using our micropipet technique but only under certain conditions. For this, a water-filled micropipet was first immersed in diluted bitumen. A droplet was then formed at the pipet tip by expelling a small amount of water into diluted bitumen, with C_0 ranging from 0.001 to 10%. Droplets thus formed were aged for 3 min. Figure 10a shows a photograph of a water droplet formed in a 0.1% bitumen. When the droplet was deflated and its area compressed, the surface crumpled abruptly (Fig. 10b), revealing a rigid cortical structure. This finding is similar to Langmuir's observations on protein films (23) and to reports on "skin" formation (9-11) at a water-crude oil interface.

The IFT isotherm in Fig. 9 suggests that, at 0.1% bitumen, there should be little or no adsorbed material on the interface. However, crumpling of the interface was observed for C_0 between 0.001 and 1%. A second anomaly is encountered when the deflation process is repeated for C_0>> 1%. As shown in Fig. 11, at high bitumen content, the interface loses its rigidity and remains spherical throughout deflation.* More interestingly, at some point during deflation, small surface protrusions begin to appear on the shrinking drop (Fig. 11b). As the interfacial area continues to decrease, these surface imperfections become more prominent and eventually detach as micrometer-sized droplets (Fig.11c). Such a process, referred to as budding, is a new emulsification mechanism, which may have important implications for the petroleum industry (24). In an industrial setting, even at gentle agitation (which cannot be avoided), water droplets would undergo various deformations and their relaxation to spherical shape would be

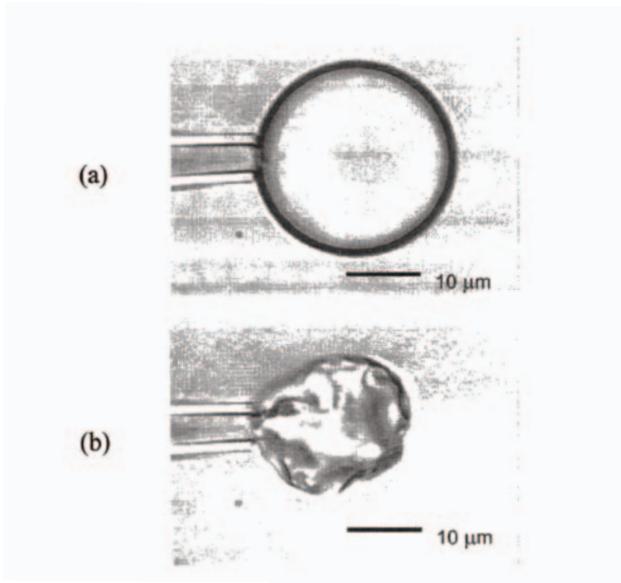

Figure 10 Deflating a water droplet below 10% bitumen in toluene solution. The initially spherical droplet (a) crumbles like a paper bag (b). Note clear background of the image.

* Transformation of the adsorbed layer from a rigid to a fluid interface (at $C_0 \approx 1$ %) does not appear abrupt.

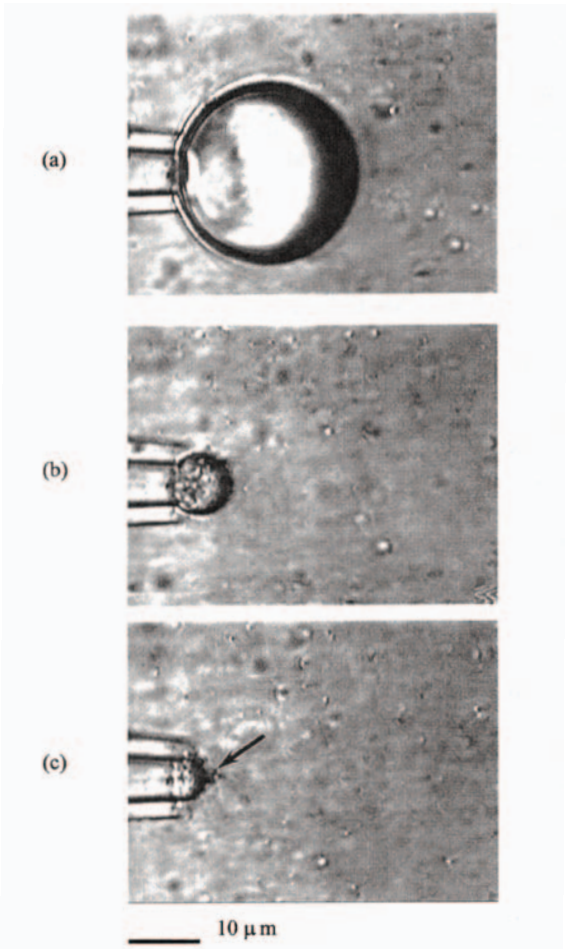

Figure 11 Deflating a water droplet above 10% bitumen in toluene solution. The droplet retains its spherical shape (a-c). At high surface compression, undulations of the interface appear (b) and grow, eventually detaching as separate much smaller droplets (c, arrow). The background is filled with small Brownian water droplets.

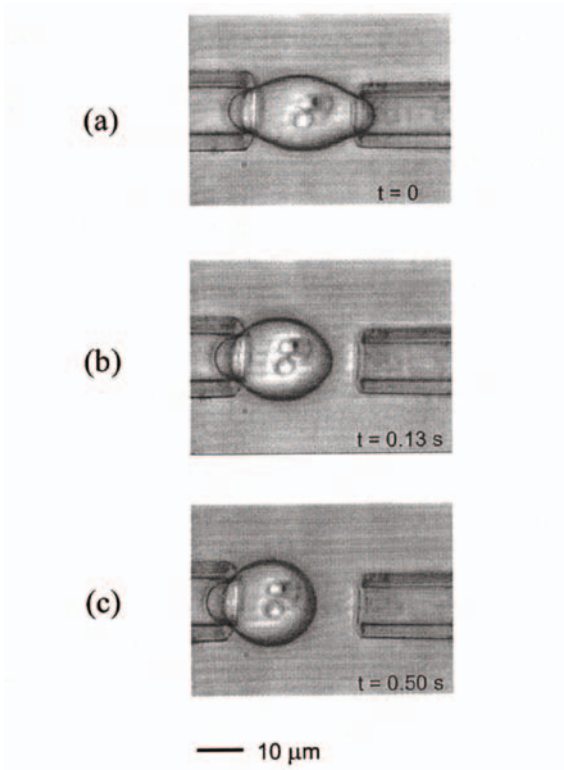

Figure 12 Kinetics of the droplet shape recovery. Description in the text.

equivalent to area compression. New emulsion droplets can thus be formed through budding at much lower shear rates than those required for a conventional droplet break-up mechanism. A detailed description of the budding mechanism has been published elsewhere (29). It is noted here that similar - although not identical - budding phenomena have been observed in biological and biophysical systems (19, 25, 26).

Adsorbed layers that crumple clearly possess resistance to surface deformations. Such resistance is manifested as surface viscosity. In a free suspension, micrometer-sized water droplets are normally spherical. Using two suction pipet as shown in Fig. 12a, such a droplet (here, formed in 0.1% diluted bitumen) is stretched and then released, thus allowing it to recover its spherical shape at constant volume (Fig. 12b,c). Typical observed times for the droplet-shape recovery are of the order of 1 s. The recovery is certainly driven by the interfacial tension σ. If the recovery process is limited by bulk viscosity, the recovery time would be of the order of

$$t_{rec} \sim \frac{\mu d}{\sigma} \qquad (2)$$

where μ is the viscosity of either water or oil (assuming they have comparable values), and d is the size of the droplet (28). Using typical values of $\mu \sim 10^3$ N. s/m^2, or σ ~ 10 mN/m and d ~10μm, the characteristic recovery time associated with bulk dissipation would be of the order of 1 μs. As the observed recovery rates are typically 10^6 times slower, the dominant source of viscous dissipation must be due to the viscosity of the adsorbed layer at the droplet surface. As suspected, these viscous effects are only observed in the crumpling regime (roughly, for $C_0 < 1$ %) where resistance to surface deformations are large. In the budding regime, the droplets recover their shape much faster. We

could not monitor the process with a video speed of 30 frames per second.

A detailed analysis of the shape-recovery experiments can be found in Ref. 29, which provides, we believe, the first measurement of interfacial transport parameters on the micrometer scale. It is noted that, although different droplets in an emulsion have uniform IFT values, their rates of shape recovery - and hence surface viscosities - appear more varied. Further study on this variability will be required.

E. Stability of Emulsion Droplets

Using the micropipet technique, two water droplets in diluted bitumen could be pressed together in an attempt to induce their coalescence (Fig. 13). At all bitumen concentrations, the emulsion drops remained stable to coalescence despite being pressed together for up to 5min. It appeared that the droplets would remain stable for much longer had the experiments continued. The flattened contact regions had radii of several micrometers. As the two droplets were separated, no sign of droplet-droplet adhesion, as indicted by the drops' elongation, was observed at bitumen concentrations below 1%. At higher concentrations, however, these signs of adhesion became visible. As expected, in control experiments involving water droplets in pure solvent, the droplets coalesced immediately on contact.

Note that at low bitumen content, where there should be very little of adsorbed material on the interface (according to the IFT isotherm in Fig. 9), the droplets already display remarkable stability. It is also interesting that, with respect to the bitumen content C_0, the detection of droplet-droplet adhesion coincides with the disappearance of interfacial crumpling. The resistance to both coalescence and adhesion at low bitumen concentration ($C_0 < 1$ %) is consistent with the steric stabilization mechanism concluded from our colloidal collider studies discussed above.

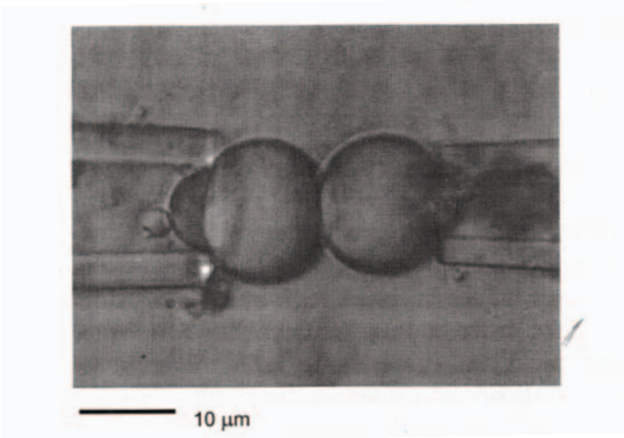

Figure 13 Resistance to coalescence. Two water droplets are pressed together in 0.1% bitumen in toluene. The compressing force, calculated from droplet shape deformation, is equivalent to about 10,000 g acceleration.

Adhesive forces which begin to appear at $C_0 > 1$ % are just above our limit of detection, which is of the order of nanonewtons. For small shape elongation (relative to the drop size), a spherical drop behaves as an elastic spring with a stiffness that is of the same order as the IFT (30). At 1 to 10% bitumen, the IFT, and hence the effective elastic constants, is ~ 10mN/m (Fig. 9). With the smallest droplet elongation that can be observed, estimated to be ~ 0.1 μm, the corresponding adhesive force is on the order of anonewtons.

The force exerted to compress the droplets is of the order of $\Delta p r^2$, where r is the radius of the contact region (about 1 μm, in our case) and Δp is the pressure difference between the droplet interior and its surrounding (roughly $10^4 N/m^2$) for a 10-μm drop. The resulting compressive force is about 10 nN. To create such forces by centrifugation, the required acceleration would have to be of the order of 10,000 g. This, as demonstrated here, would still be futile in causing coalescence in agreement with our observations. When we centrifuge our emulsions, even at 20,000 g, we can separate creamed emulsion in the form of a cake, without breaking the emulsion into separate water and oil phases.

The Marangoni effect, that is, the retardation of thin-film drainage by induced tension gradients, is believed to play an important role in emulsion stabilization (31). The most "severe" case of Marangoni's effect is, of course, one that involves immobile surfaces. The associated drainage time can be estimated from the Reynolds equation (31):

$$\frac{d}{dt}\left(\frac{1}{h^2}\right) = \frac{4}{3}\frac{\Delta p}{\mu r^2} \qquad (3)$$

where H is the film thickness, μ is the viscosity of diluted bitumen (roughly that of water), and Δp and r have the same meaning and values as stated above. Assuming that, as h falls below 1 nm, film drainage is greatly accelerated by attractive colloidal forces, the corresponding film drainage time is of the order of 0.1s. Yet, the water droplets in our studies remain stable for minutes or longer under the same drainage forces. It thus appears that the Marangoni effect is

not the dominant stabilizing mechanism in water-in-diluted bitumen emulsions.

V. THIN-FILM STUDIES: PROPERTIES OF THIN EMULSION FILM IN WATER-DILUTED BITUMEN-WATER SYSTEM

As the two water droplets of a W/O emulsion approach each other a thin oil film is formed between them (Fig. 14a). For the droplets to coalesce, this oil film has to break. Such a film can be created inside a specially designed measuring cell (32) of the thin liquid film-pressure balance technique (TLF-PBT) (Fig. 14b). Due to the curvature of the oil-water interface, a capillary pressure arises at the edge of the film, forcing the liquid to drain from the film. As the film becomes thinner, the interfaces which bind the film begin to interact through van der Waals, electrostatic, steric, or other surface forces. The overall effect of all these forces, which is known as disjoining pressure, determines whether the film will remain stable and thus directly determines the stability of the emulsion. The principle of the measuring technique involves balancing the capillary pressure with the film disjoining pressure. Although the technique has been extensively used for studies of foams, relatively little work has been done on emulsion films and even less on water-oil-water systems. The first attempt at applying this technique to study water-diluted bitumen-water system was made in Wasan's laboratory in Chicago, (33). Later on, a thin-film instrument was set up in our laboratory. A detailed description of our experimental set-up and procedures can be found in Ref. 34.

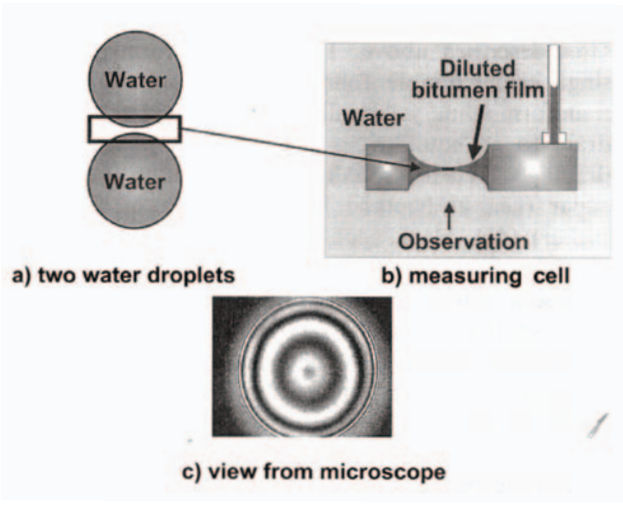

Figure 14 Schematic of thin-film technique. The geometry of the oil film separating two water droplets (a) is recreated in a special holder in the thin-film measuring cell (b); (c) shows microscopic image at the beginning of the film-thinning process showing Newton interference rings.

As in the previous sections, the objective of this study was to obtain insight into the mechanisms that stabilize water in dilute bitumen emulsion with particular attention to the relative importance of the resin, asphaltene, and solids fractions of the bitumen.

A. Experimental

Our experimental set-up is described in detail in Ref. 34. The porous-plate measuring cell was placed inside a thermostated jacket on a Carl Zeiss Axiovert 100 inverted microscope. The film was viewed and recorded with a CCD video camera and a VCR. The capillary pressure was controlled by adjusting the height of the solution, using a manually operated micrometer syringe or by adjusting the air pressure inside the cell.

The film thickness was determined by a microinterferometric method (33-37) using heat-filtered light from a 100-W mercury-arc lamp and a monochromatic filter (λ. = 546 nm). The incident light was directed through a pinhole or iris diaphragm creating a ~ 10 μm spot focused on the center of the film. The intensity of reflected light passing through a second pinhole diaphragm was measured with a low-light, low-noise photodiode and recorded using a chart recorder. The equivalent thickness, h, was calculated following the procedure developed by Scheludko and Platikanov (38), assuming that the film was optically homogeneous with the refractive index of the film equal to the refractive index of the solvent used to prepare the bitumen solution studied.

Syncrude's coker feed bitumen, which was used for all experiments, had already been treated in commercial plant operations to remove coarse sand and water and was ready for upgrading. Deasphalted bitumen (i.e., bitumen with asphaltenes and solids fractions removed) was obtained by diluting coker feed bitumen with heptane to a volume ratio of 40:1 (heptane: bitumen), filtering the supernatant after 24 h and stripping the diluent by evaporation at 60°C to constant mass. The asphaltene fraction was recovered from the precipitate by dissolving it with toluene, centrifuging, and evaporating the solvent as before. The resin fractions (I and II) of bitumen were obtained using the SARA method (39) although only resin fraction I was used in the thin-film measurements. Solids-free bitumen was prepared by dilut-

ing coker feed bitumen with toluene to a volume ratio of 100:1 (toluene: bitumen), centri-fuging at 20,000 g, filtering through a Millipore 22-μm filter, and stripping the solvent to a constant mass. HPLC-grade toluene and n-heptane were used to prepare all solutions. Three separate samples were prepared at each weight ratio and were used immediately after preparation to avoid any possible aging effects. All films were immersed into a solution of 0.014 M sodium chloride, 0.012 M sodium bicarbonate, and 0.04 M sodium sulfate (ph ~ 8.2) to imitate the composition of water used in Syncrude's commercial operation.

B. Results

1. Toluene-diluted Bitumen Films

Figure 15a displays a series of images of the typical drainage pattern for a toluene-diluted bitumen film, from the stage of formation to the equilibrium gray film. A single center dimple appeared upon initial film formation; the liquid in the dimple would drain off through channels until a uniform white/yellow film was reached. The film would then continue to drain slowly via plane-parallel drainage to an equilibrium gray film. At high diluent/bitumen ratios (10 : 1 to 20:1), several "blurry" white dimples of trapped liquid approximately 3 to 5 /xm in diameter often appeared in the dark gray films similar to those observed by Bergeron et al. in hydrocarbon foam films (40). The rate of film drainage was limited by the bulk viscosity of the bitumen solution.

Figure 16 (curve 2), depicts the experimentally obtained thickness for toluene-diluted bitumen emulsion films. At an industry-relevant diluent ratio of about 1:1 toluene to bitumen, the film thickness values scattered within a large range from about 50 to 60 nm. These films required long periods of time to reach equilibrium, and the film diameter would fluctuate resulting in a large variation in the measured film thickness. Such a film probably had a multilayer structure.

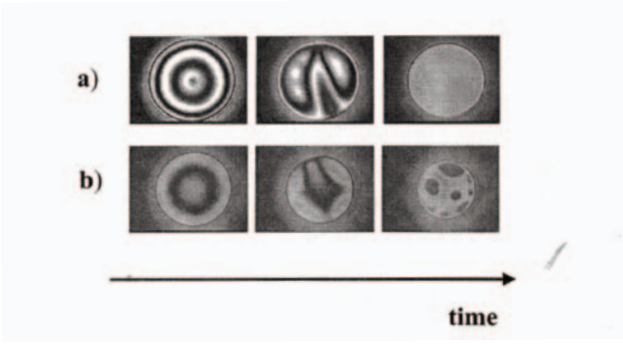

Figure 15 Film-thinning process for bitumen in toluene (a) leads to a relatively thick gray film. For bitumen in heptane solution, thinning leads to formation of black spots, which eventually coalesce forming a thin black film (b).

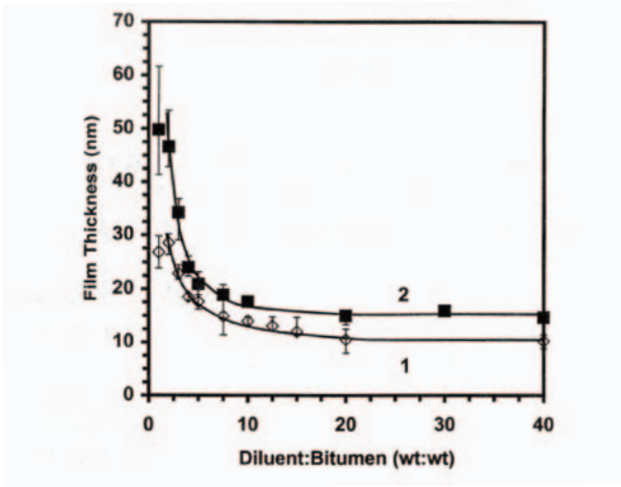

Figure 16 Film thickness for bitumen in heptane (1) and bitumen in toluene (2) solutions for various diluent-to-bitumen ratios.

2. Heptane-diluted Bitumen Films

With no asphaltene precipitation (i.e., at 1:1 heptane : bitumen ratio where no asphaltene precipitation occurs), the behaviour of a heptane-diluted bitumen film was very similar to that of toluene-diluted bitumen films described above. The film was formed with a single center dimple, followed by channel drainage to a uniform white/yellow film, which would continue to drain to an equilibrium gray film via plane-parallel drainage. When asphaltene precipitation began to occur (i.e., at heptane: bitumen ratios of 1.7:1 or higher) (41), black spots would appear within 5 to 10 s after film formation (Fig. 15b). The spots quickly coalesced in to a uniform black film with several small white spots of about 1 to 3 /xm in diameter similar to the dimples observed by other researchers (40, 42, 43). A slight decrease in film thickness was observed once the black film had been formed. About half an hour after loading the cell, small aggregates of asphaltene precipitate began to appear near the oil/water interface. The aggregates were approximately 5 to 10μm in diameter, which was close to the mean particle size of 7.0 ± 4.0 μm reported by Li and Wan (44). Over time (> 2h), the number of asphaltene aggregates would continue to increase until any newly formed film

would become completely clogged, preventing it from draining.

The stability of the heptane/bitumen emulsion films depended strongly on the diluent ratio. At a ratio of 1:1, the film remained stable for at least an hour while films of 2:1 to 3 :1 dilution remained stable for at least 20min. The stability of the film then dramatically decreased with increasing diluent ratio, causing the film lifetime to fall to less than 25 s for ratios of 20:1 or more (Fig. 17).

The thickness measurements for the heptane-diluted bitumen films are presented in Fig. 16 (curve 1). Below the onset of asphaltene precipitation at a heptane/bitumen ratio of about 1:1, the film drained to an equilibrium gray film of about 27 nm thickness. Above the precipitation onset at a heptane/bitumen ratio of 2:1, the black film reached a thickness of about 28 nm. The film thickness then decreased with increasing diluent: bitumen ratio to about lOnm at a ratio of 20:1. The thickness then remained constant, indicating that a bilayer film was probably reached. At lower diluent ratios (< 20 : 1), the greater thickness of heptane/bitumen films may be caused by the presence of unprecipitated asphaltenes.

A comparison of the thickness of both heptane- and toluene-diluted films (Fig. 16, curves 1 and 2, respectively) indicated a consistently lower thickness for the former films. One would expect that the presence of the resins, asphaltenes, and solids fractions determined the thickness and behaviour of the emulsion films. The effect of each fraction can be isolated to determine which fraction(s) dominated the film behaviour in each solvent.

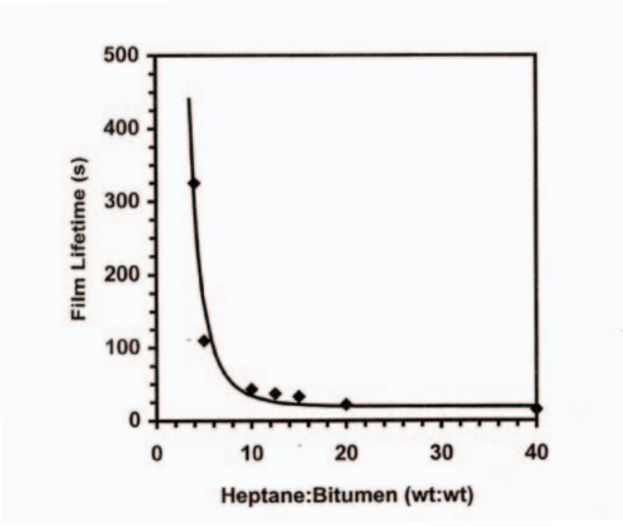

Figure 17 Film lifetime for bitumen in heptane solutions.

3. Solids-free Bitumen

Fine solids are frequently mentioned as being responsible for W/O emulsions, especially in systems involving various crude oils. The solids fraction of bitumen consists of fine submicrometer clay particles that have been rendered "asphaltene-like" due to the adsorption of highly aromatic, polar material on the particle surfaces (45). To determine if this solid fraction played a role in the film stability, a "solids-free" bitumen was prepared where all solid material larger than lOOnm was removed from the sample. Films of toluene- and heptane-diluted solids-free bitumen showed little or no change in both the drainage patterns and the film thickness, indicating that the fine solids had little or no effect on the behaviour or stability of water/diluted bitumen/water films. This is consistent with the observation described in Sec. II, where removal of fine solids from diluted bitumen had no effect on subsequently formed water in diluted bitumen emulsion.

Solid particles were observed at or near the oil-water interface on several occasions in toluene-diluted bitumen films. The particles were easily pushed away from the film into the meniscus region when the films were first formed and never appeared in the film itself. For the solids fraction to play a role in emulsion stability, we thus expect that the fine clay particles probably build up in the Plateau borders around water droplets and clog the drainage routes through the emulsion, contributing to its additional, kinetic stability. Therefore, it may be expected that the fine solids may have a contribution to the overall W/O emulsion stability, but this is not the leading factor.

4. Resins

The effect of the resins was studied by observing a number of thin films of diluted deasphalted bitumen (i.e., free of asphaltene and solid fractions) and diluted resins I. Most of the experiments were conducted using deasphalted bitumen because of the high cost and long time needed to isolate a small amount of resin I through the SARA method (39). The properties of deasphalted bitumen and resin-I films in either toluene or heptane solutions were similar to the heptane-diluted bitumen films with a black film being formed via black spots. The film thickness was also independent of the solvent type, ranging from 14nm at a dilution of 1:1 to 12 nm for a 10:1 diluent ratio. Experiments with resin I diluted to 5:1 and 10:1 in toluene displayed similar drainage patterns to those of the deasphalted bitumen films and a nearly identical film thickness.

These results indicate that the resin fraction determined the properties of heptane-diluted bitumen films at high diluent ratios. Since the thickness remained constant with further dilution, the film probably had a bilayer structure. The relative instability of heptane-diluted bitumen, deasphalted bitumen, and resin-I films agree well with the emulsion experiments of Yan (46) where deasphalted bitumen led to poorly stabilized water-in-bitumen emulsions.

5. Asphaltenes

Since asphaltenes have been identified as the most common stabilizers of water-in-bitumen emulsions (47), we expected that the asphaltenes could be responsible for the stability of the toluene-diluted bitumen films. A single experiment on a film of toluene-diluted asphaltenes at a weight ratio of 15 :1 followed a similar drainage pattern to that of the toluene-diluted bitumen films with a uniform gray film being formed. However, the film unexpectedly ruptured after only a few minutes at a thickness of 36 nm. McLean and Kilpatrick (48) showed that stable water-in-oil emulsions could be obtained with pure asphaltenes. They also found that the combination of resin and asphaltene at a ratio of 1: 3 (resin: asphaltene) resulted in the most stable emulsions. A thin film of resin I and asphaltene diluted in toluene (2: 1 resin I: asphaltene by weight) displayed very similar behavior to the toluene-diluted bitumen films with slow drainage to a stable gray film. The equilibrium thickness of the resin I: asphaltene film was also very similar to the thickness of the toluene-diluted bitumen films. These results indicated that the combined interaction of resins and asphaltenes are important to the film stability. Again, it is worth noting that the conclusion from the washing experiments discussed above was that it is not the whole asphalthene fraction that is involved but only a small subfraction of the total asphalthene present in the oil. We are not sure what the chemical characteristics of this "bad actor" are.

While the asphaltene and resin fractions alone provide a partially stable film, the combination of resin and asphaltene produce extremely stable films. However, additional information is needed to confirm our assumptions that the films have a multilayer structure at lower diluent ratios and a bilayer structure at high diluent ratios. We hope that future measurements of the disjoining pressure-thickness isotherms will provide this confirmation as well as identify the surface forces that stabilize the water/diluted-bitumen/water films.

Bitumen is a complex mixture of hydrocarbons that can be divided into several material classes based on solubility. The classes include saturates, aromatics, resins, and asphaltenes. Asphaltenes are generally defined as the bitumen fraction that is soluble in toluene and insoluble in an aliphatic solvent. In the case of heptane, large asphaltene molecules begin to precipitate at a heptane: bitumen volume ratio of around 1.4:1 to 1.7:1 (48) with complete asphaltene precipitation occurring at volume ratios above 40:1. The asphaltene molecules are polyaromatic hydrocarbons that consist primarily of aromatic clusters and aliphatic chains along with a variety of functional groups (50, 51). Resins consist of similar chemical species except the molecules, on average, have a lower molar mass, fewer functional groups, and a higher H/C ratio. It is well known that asphaltenes play a significant role in the stability of the water-in-bitumen emulsions (48, 52-55). Resins are considered to be surface active (49, 52, 56) and, to a limited extent, are capable of stabilizing an emulsion. McLean and Kilpatrick have shown that the combination of resin and asphaltene at a ratio of around 1: 3 (resin: asphaltene by weight) provide the most stable emulsions (48). The bitumen extracted from oil sands also contains very fine solids composed of clay particles coated with strongly bound toluene-insoluble organic material. These solids are also suspected of playing a role in water-in-oil emulsion stability (45, 46).

VI. SUMMARY

Water-in-diluted bitumen emulsion is characterized by high stability, creating serious operational problems in commercial operations. Our studies indicate that this stability is due to an adsorbed layer at the water-oil interface responsible for a steric barrier to droplet coalescence. This steric repulsion was detected by using the colloidal collider technique, new tool for studying surface-to-surface interactions between particles or droplets of several micrometers size. The protective "skin" formed at the droplet surfaces was visualized by deflating water droplets formed at the tip of a micropipet. (The micropipet experimental technique was borrowed from biological studies, where it is commonly used to manipulate individual cells.) The deflating water droplets in diluted bitumen solutions in toluene (below 1 wt%) crumble like paper bags, indicating that the surface layer is rigid. At higher concentrations, the surface layer becomes highly flexible. As a result, the deflating droplets remain spherical, but instead of crumbling they spawn smaller droplets through a new spontaneous emulsiflcation

mechanism. This spontaneous emulsification may be responsible for formation of W/O emulsions in many oil industry related systems.

The transition from crumbling to spawning regime occurs at a characteristic bitumen in diluent concentration, which depends on the paraffinic/aromatin nature of the solvent. The higher solvent aromaticity, the higher is this transition concentration. Above this critical concentration, a very persistent emulsion is easily formed, no doubt partially through the spontaneous emulsification mechanism mentioned above. Below the critical concentration (or at higher diluent-to-bitumen ratios) a clean, dry oil phase can be produced using inclined plate settlers or centrifuges. For a paraffinic diluent, like heptane, or natural gas condensate, this transition takes place at bitumen-to-solvent ratio of about 2, allowing for development of a commercial paraffmic diluent technology.

Thin-film studies confirmed observations from other techniques. Among others, they revealed that the film separating two water droplets in heptane-diluted bitumen is about half the thickness when toluene is used as a solvent. Also, the film lifetime is considerably shorter in a paraffin-based system. Demulsifiers that are used in industry to lower the water content in the feed to refineries compete for the water-oil interface with a substance or substances that produce the protective steric layers.

It is still unknown what the mechanism is behind the transition from rigid to flexible character of the layer on the water-oil interface mentioned above. There is a strong possibility that a phase transition takes place there, most likely of a type known for microemulsion systems. An attempt at getting some insight into the phase equilibria in the system of bitumen, diluent, water, and perhaps added surfactants (demulsifiers) will be the subject of our future studies.

ACKNOWLEDGMENTS

The research reported in this chapter was done in close collaboration between the NSERC Industrial Research Chair in Oil Sands at the University of Alberta, CANMET Western Research Centre, and Syncrude Research Centre in Edmonton. Natural Science and Engineering Research Council of Canada (NSERC) support to the above-mentioned Chair is greatly acknowledged. The author wishes to thank Syncrude Canada Ltd for the permission to publish this material and his colleagues and friends: Tad Dabros, Khristo Khristov, Jacob Masliyah, Kevin Moran, Shawn Taylor, Alex Wu, and Tony Yeung for providing the data, artwork, and numerous discussions, and for their help in preparation of the manuscript.

REFERENCES

1. YXuJ Dabros, H Hamza, B Shelfantook. Petrol Sci Technol 17: 1051—1070, 1999.
2. TGM van de Ven, P Warszynski, X Wu, T Dabros. Langmuir 10: 3046—3056, 1994.
3. X Wu, TGM van de Ven. Langmuir 12: 3859—3865, 1996.
4. X Wu, TGM van de Ven, J Czarnecki. Colloids Surfaces A 149: 577—583, 1999.
5. JH Schenkel, JA Kitchener. Trans Faraday Soc 56: 161—173, 1960.
6. J Visser. Adv Colloid Interface Sci 3: 331—363, 1972.
7. X Wu, TGM van de Ven. J Colloid Interface Sci 183: 388—396, 1996.
8. RH Yoon, D Guzonas, BS Aksoy. Processing of hydrophobic minerals and fine coal. Proceedings of the First UBC-McGill Bi-Annual International Symposium, Vancouver, 1995, pp 277-289.
9. CG Dodd. J Phys Chem 64: 544—550, 1960.
10. FE Bartell, DO Niederhause. Research on Occurrence and Recovery of Petroleum. New York: American Petroleum Institute, 1949, pp 57-80.
11. JE Strassner. J Petrol Technol 20: 303—312, 1968.
12. OK Kimbler, RL Reed, IH Silberg. Soc Petrol Eng I 6: 153—165, 1966.
13. A Yeung, T Dabros, J Masliyah. J Colloid Interface Sci 208: 241—247, 1998.
14. EA Evans, R Skalak. Mechanics and Thermodynamics of Biomembranes. Boca Raton, FL: CRC Press, 1980.
15. E Evans, D Needham. J Phys Chem 91: 4219—4228, 1987.
16. A Yeung, E Evans. Biophys J 56: 139—149, 1989.
17. A Yeung, T Dabros, J Masliyah. J Colloid Interface Sci 208: 241—247, 1998.
18. RC Shaw, LL Schramm, J Czarnecki. In: LL Schramm, ed. Suspensions: Fundamentals and Applications. Washington, DC: American Chemical Society, 1996, pp 639-675.
19. E Evans, W Rawicz. Phys Rev Lett 64: 2094—2097, 1990.
20. N Cyr, DD Mclntyre, G Toth, OP Strausz. Fuel 66: 1709—1714, 1987.
21. A Bhardwaj, S Hartland. Ind Eng Chem Res 33: 1271—1279, 1994.
22. SE Taylor. Fuel 71: 1338—1339, 1992.

23. I Langmuir, DF Waugh. In: CG Suits, HE Way, eds. The Collected Works of Irving Langmuir. Vol 7. New York: Pergamon Press, 1961, pp 27-35.
24. T Dabros, A Yeung, J Masliyah, J Czarnecki. J Colloid Interface Sci 210: 222—224, 1999.
25. B Alberts, D Bray, J Lewis, M Raff, K Roberts, J Watson. Molecular Biology of the Cell. New York: Garland Publishing, 1989.
26. R Lipowsky. Nature 349: 475—481, 1991.
27. A Yeung, T Dabros, J Masliyah, J Czarnecki. Colloids Surfaces A 174: 169—181, 2000.
28. A Yeung, E Evans. J Phys II France 5: 1501—1523, 1995.
29. A Yeung, T Dabros, J Czarnecki, J Masliyah. Proc Royal Soc A, 445: 3709—3723, 1999.
30. E Evans, K Ritchie, R Merkel. Biophys J 68: 2580—2587, 1995.
31. DA Edwards, H Brenner, DT Wasan. Interfacial Transport Processes and Rheology. Boston: Butterworth-Heinemann, 1991.
32. D Exerowa, A Scheludko. Compt Rend Acad Bulg Sci 24: 47—50, 1971.
33. A Nikolov, D Wasan, J Czarnecki. Presented at 47th Canadian Chemical Engineering Conference, Edmonton, 1997.
34. K Khristov, S Taylor, J Czarnecki, J Masliyah. Colloids Surfaces A 174: 183—196, 2000.
35. D Exerowa, PM Kruglyakov. Foam and Foam Films. New York: Elsevier, 1998.
36. A Scheludko. Kolloid Z 155: 39^4, 1957.
37. A Scheludko. Adv Colloid Interface Sci 1: 391—464, 1967.
38. A Scheludko, D Platikanov. Kolloid Z 175: 150—158, 1961.
39. JT Bulmer, J Starr, eds. Syncrude Analytical Methods for Oil Sand and Bitumen Processing. Edmonton: Syncrude Canada Ltd, 1979, pp 121-124.
40. V Bergeron, JE Hanssen, FN Shoghl. Colloids Surfaces A 123/124: 609—622, 1997.
41. PF Clarke, BB Pruden. Petrol Sci Technol 16: 287—305, 1998.
42. JL Joye, CA Miller, GJ Hirasaki. Langmuir 8: 3083—3092, 1992.
43. Y Horiuchi, H Matsumura, K Furusawa. J Colloid Interface Sci 207: 41—45, 1998.
44. H Li, WK Wan. International Heavy Oil Symposium, Calgarry, 1995, pp 709-716.
45. LS Kotlyar, BD Sparks, JR Woods, S Raymond, Y LePage, W Shelfantook. Petrol Sci Technol 16: 1—19, 1998.
46. Z Yan. Interfacial behaviour of de-asphalted bitumen. MSc dissertation, University of Alberta, Edmonton, 1997.
47. HW Yarranton. Asphaltene solubility and asphaltene stabilized water-in-oil emulsions. PhD dissertation, University of Alberta, Edmonton, 1997.
48. JD McLean, PK Kilpatrick. J Colloid Interface Sci 196: 23—34, 1997.
49. PF Clarke, BB Pruden. Petrol Sci Technol 16: 287—305, 1998.
50. OP Strausz, TW Mojelsky, EM Lown. Fuel 71: 1355—1363, 1992.
51. DL Mitchell, JG Speight. Fuel 52: 149—152, 1973.
52. JD McLean, PK Kilpatrick. J Colloid Interface Sci 189: 242—252, 1997.
53. EJ Johansen, IM Skjärvö, T Lund, J Sjöblom, H Söderlund, G Boström. Colloids Surfaces 34: 353—370, 1988/89.
54. MH Ese, J Sjöblom, H Førdedal, O Urdahl, HP Rønningsen. Colloids Surface A: 123/124: 225—232, 1997.
55. O Mouraille, T Skodvin, J Sjöblom, JL Peytany. J Dispers Sci Technol 19: 339—367, 1998.
56. EH Sheu, OC Mullins, eds. Asphaltenes: Fundamentals and Abdications. New York: Plenum Press, 1995.